Pure Appl. Chem., Vol. 84, No. 10, pp. 2027–2043, 2012.
http://dx.doi.org/10.1351/PAC-CON-11-10-10

Chemiluminescence immunoassay for a nonionic surfactant using a compact disc-type microfluidic platform*

Shuai Guo[1], Koji Nakano[1], Hizuru Nakajima[2], Katsumi Uchiyama[2], Akihide Hemmi[3], Yoshikazu Yamasaki[4], Shigeharu Morooka[4], Ryoichi Ishimatsu[1], and Toshihiko Imato[1,‡]

[1]Department of Applied Chemistry, Graduate School of Engineering, Kyushu University, Fukuoka, 819-0395, Japan; [2]Department of Applied Chemistry, Graduate School of Engineering, Tokyo Metropolitan University, Tokyo, 192-0397, Japan; [3]Mebius Advanced Technology Ltd., Tokyo, 167-0042, Japan; [4]Department of Chemical Engineering, Faculty of Engineering, Fukuoka University, Fukuoka, 814-0180, Japan

Abstract: A simple and pump-free chemiluminescence immunoassay based on a compact disc (CD)-type microfluidic platform for the determination of alkylphenol polyethoxylates (APnEOs) is described. The method is based on a competitive immunoreaction of the anti-APnEOs antibody immobilized on the magnetic microbeads between APnEOs and horseradish peroxidase (HRP)-labeled APnEOs in the sample solution. The luminol solution containing H_2O_2 and enhancer is caused to flow from one reservoir in the platform to another by appropriate adjustment of the speed of the rotation of the disc. The detection limit was similar to that reported in our previous paper, i.e., 10 ppb according to IC_{80}.

Keywords: bioanalytical methods; binding constants; chemiluminescence immunoassay; compact disc (CD)-type microfluidic platform; enzyme chemistry; green chemistry; magnetic microbeads; optical emission spectroscopy.

INTRODUCTION

Alkylphenol polyethoxylates (APnEOs), which are classified as nonionic surfactants, have been used worldwide for more than 50 years domestically and in industrial processes such as petroleum amelioration, metal working processes, and pulp and paper production, as well as the manufacture of plastics. Their widespread use can be attributed to the unique properties associated with their molecular structures, which are composed of a polyethoxy chain and an alkyl chain connected to a benzene ring. The chains are broken down in wastewater treatment plants during biological treatment, and the resulting metabolites such as short-chained APnEOs (n = 1–3), alkylphenol polyethoxycarboxylates, carboxyalkylphenol polyethoxycarboxylates, and alkylphenol [1–2] are discharged into environmental water with the treated water from the plants. APnEOs and their metabolites can bind to soils and sediments and bioaccumulate in plants and animals, and are suspected of having estrogenic activity in

Pure Appl. Chem. **84**, 1973–2063 (2012). A collection of invited papers based on presentations on the Novelty in Green Analytical Chemistry theme at the 14th Asian Chemical Congress (14 ACC), Bangkok, Thailand, 5–8 September 2011.
‡Corresponding author: E-mail: imato@cstf.kyushu-u.ac.jp

wildlife and humans by interacting with estrogen receptors in living cells [3–7]. This is a matter of great public concern, in view of their threat as potential endocrine disrupters. Therefore, a rapid and sensitive analytical method for the determination of APnEOs would be highly desirable, especially in areas where water is discharged from wastewater treatment plants.

Many reports concerning the determination of APnEOs using traditional analytical methods, such as gas chromatography-tandem mass spectrometry [8,9], liquid chromatography-tandem mass spectrometry [10–13], high-performance liquid chromatography [14–18], matrix-assisted laser desorption/ionization mass spectrometry [19], and capillary electrochromatography-electrospray ionization-mass spectrometry [20] have appeared, and all of these methods are sensitive and reliable. Since APnEOs and their metabolites are comprised of fragments with various chain lengths and functional groups, samples intended for analysis must be pretreated, which makes the overall process time-consuming and complicated. These procedures constitute drawbacks to the above methods. Moreover, the instrumentation used is expensive and a high degree of skill is required of the technicians who are responsible for the analyses. In contrast to these methods, a method based on an enzyme-linked immunosorbent assay (ELISA) for the determination of APnEOs would be simple, rapid, and inexpensive and would not require expensive instrumentation [21,22]. One of the disadvantages of this method is that many procedures, such as the addition of sample and reagents, washing and bound/free (B/F) separation are required. In our previous work, in an attempt to automate the above ELISA method for the determination of APnEOs, we proposed a sequential injection chemiluminescence immunoassay that involved the use of magnetic microbeads [23]. If the sequential injection system, including the pumping system, could be integrated into one small microchip, it would be possible to drastically miniaturize the process.

A compact disc (CD)-type microfluidic platform has recently attracted interest for potential use in a micro-total analytical system. Such a platform would be versatile and would have widespread applicability for many analytical purposes, such as cell lysis and metering [24–27], DNA assays [28–32], immunoassays [33–35], single nucleotide polymorphism (SNP) detection [36], and the detection of hemoglobin [37]. In addition to the advantages of such a microfluidic device, which includes a reduction in sample volumes and short diffusion length for the reagent due to the use of microscale-sized reservoirs and channels, the CD-type microfluidic platform has the advantage that the pumping function is integrated, and, moreover, the sequence of flow can be controlled by the speed of rotation of the platform. Namely, several reservoirs for sample and reagent solutions and some reservoirs for reactions and detection are linked by microchannels on the CD-type microfluidic platform. As a result, by rotating the platform on a turntable, the centrifugal force functions as a pump, causing the solutions in the reservoir to flow to the reservoir for reaction and detection, and the sequence of flow can be controlled by the speed of rotation of the platform. In this paper, we describe a portable analytical system that can be used for the determination of APnEOs in environmental water samples via the use of a CD-type microfluidic platform based on a chemiluminescence immunoassay. The proposed method appears to have great potential for use in point-of-care monitoring of water quality in wastewater treatment plants.

EXPERIMENTAL

Analytical system

Figure 1 shows the instrumental set-up used in this study. The CD-type microfluidic platform is a two-layered structure; the first layer is made of polydimethylsiloxane (PDMS) with reservoirs and microchannels, and the second is made of polycarbonate coated with a thin PDMS film, with a permanent magnet ($\phi = 4$ mm, 2.5 mm in thick) at the same position as the reservoir for the reaction and detection of the PDMS layer. The magnetic microbeads coated with polylactic acid (particle size: 100 μm in diameter) were placed in the reservoir and fixed by a permanent magnet embedded in the polycarbonate platform. The CD-type microfluidic platform was placed on a turntable, and the speed of rotation

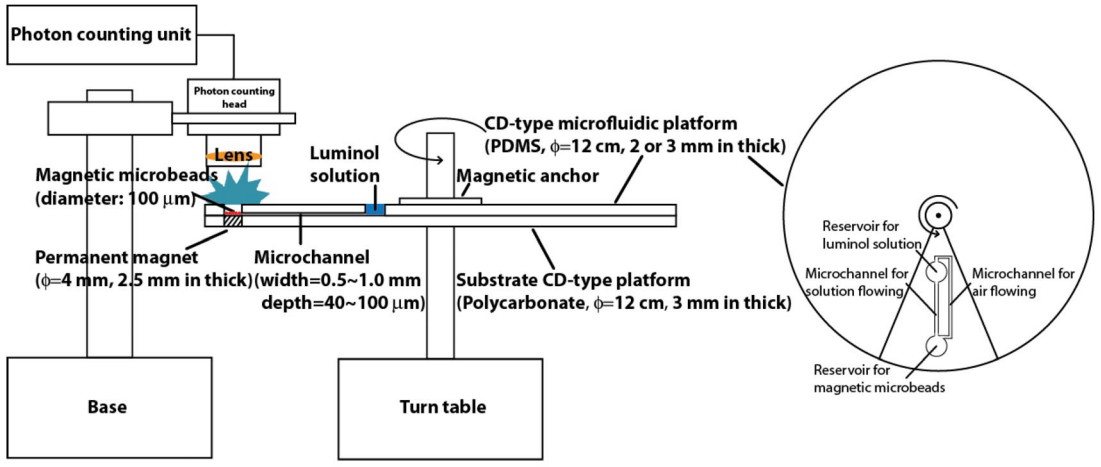

Fig. 1 The analytical system constructed from a CD-type microfluidic platform and a photon counting unit.

was controlled by adjusting the applied voltage, which was programmed by a LabView software program on a personal computer. A calibration plot of rotation speed vs. applied voltage was preliminarily prepared using a stroboscope. A photon counting unit as a detector of chemiluminescent light (C8855, Hamamatsu Photonics Co., Japan) was fixed above the reservoir where the magnetic microbeads were located. The entire system was placed in a dark chamber to eliminate any effects of ambient light.

Materials and reagents

An anti-APnEOs monoclonal antibody and horseradish peroxidase (HRP)-labeled APnEOs were obtained from Tokiwa Chemicals Industries Co. (Japan). Magnetic microbeads coated with polylactic acid (OLA-particles-M COOH, particle size: 100 μm) were obtained from Micromod Co. (Germany). The magnetic microbeads were supplied as a suspension at a concentration of 10 mg mL^{-1}. Luminol, HRP, Tween 20, *N*-hydroxysuccinimide (NHS), and 1-ethyl-3-(3-dimethylaminopropyl) carbodiimide hydrochloride (EDC) were purchased from Wako Chemical Co. (Osaka, Japan). All the reagents were obtained commercially and were used without further purification.

Preparation of CD-type microfluidic platform

The silicon template for preparing the upper layer of the CD-type microfluidic platform was fabricated by a photolithography method. A thin photoresist (SU 8, Nippon Kayaku Co., Japan) film was formed on the surface of a silicon wafer (6 inches in diameter, Sumco Co., Japan) by spin coating. After heating (e.g., at 65 °C for 5 min followed by at 95 °C for 45 min) on a hot plate, the silicon wafer was covered with a transparent photo mask prepared using an inkjet printer, and was exposed to UV light in a light box (Model Box W9B, Sunhayato Co., Japan). After another heating (e.g., at 65 °C for 1 min followed by at 95 °C for 5 min) on a hot plate, the silicon wafer was then rinsed in a developer solution to remove the unexposed part covered by the photo mask. Finally, the silicon wafer was heated again at 150 °C to harden the remaining photoresist. The resulting template prepared on the silicon wafer was placed in a container made of an acrylic resin plate with a space of 2 mm in thickness, where a prepolymer of PDMS containing its cross-linker at a weight ratio 10:1 was poured into, to prepare a mold. The molded PDMS was heated at 80 °C in an oven for 6 h and then detached from the silicon wafer. Finally, the PDMS mold was cut accurately to fit to the design, and the reservoirs were cut using

circular-type cutters with corresponding diameters, and the PDMS layer was attached to the lower layer of the polycarbonate substrate.

Measurement of critical rotation speed for CD-type microfluidic platform

Figure 2 shows an illustration of a part of the CD-type microfluidic platform and the forces exerted on a solution at the outlet of the reservoir. The centrifugal force exerted on the solution in the reservoir causes it to flow out into the microchannel by rotating the platform, while the surface tension prevents the solution in the reservoir from flowing out, since the surface of the PDMS platform is hydrophobic. The centrifugal force is expressed as eq. 1:

$$F_c = R\omega^2 \rho A h \tag{1}$$

where R, A, and h denote the distance between the channel inlet and the center of the platform, the area of the cross-section of the microchannel and the height of the solution, respectively. ω and ρ denote the angular velocity of the rotation and the density of the solution, respectively. The surface tension is expressed as eq. 2:

$$F_s = C\gamma\cos\theta \tag{2}$$

where C, γ, and θ are the perimeter of the cross section of the microchannel, the surface tension of the solution and the contact angle between the solution and the surface, respectively.

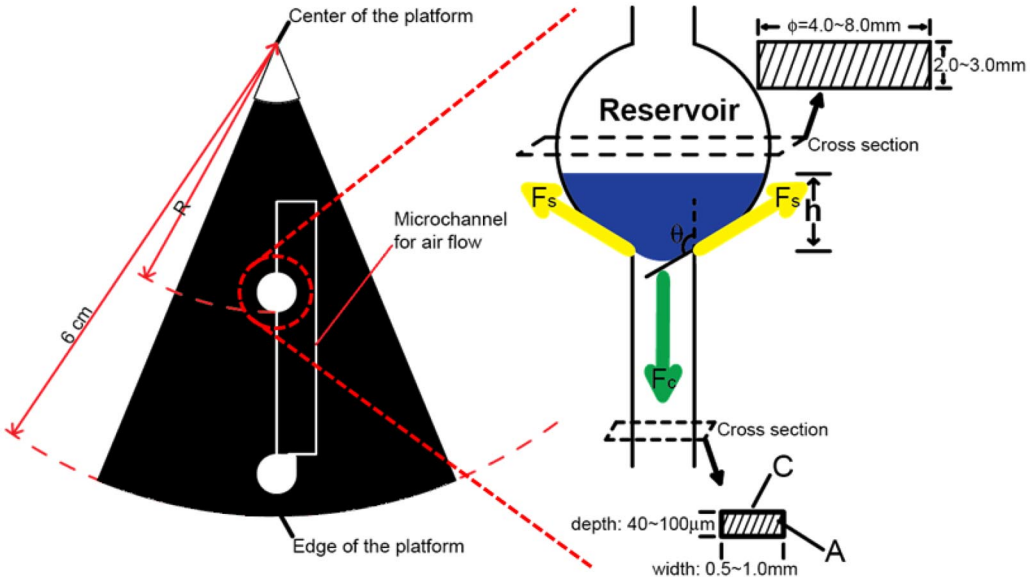

Fig. 2 Scheme showing the reservoirs for a luminol solution and for magnetic microbeads linked with a microchannel, and the centrifugal force and surface tension exerted on the solution at the outlet of the reservoir.

Equation 2 indicates that the surface tension is independent of the rotation speed. The surface tension acts as a valve, since its direction of force is opposite that of the centrifugal force. The centrifugal force increases when the rotation speed is increased, and at the critical point, the centrifugal force becomes equal to the surface tension. The critical rotation speed, ω_c expressed in rpm units, is derived by equating the centrifugal force to the surface tension as eq. 3:

$$\omega_c = \frac{60}{2\pi}\sqrt{\frac{C\gamma|\cos\theta|}{AR\rho h}} = \frac{60}{\pi}\sqrt{\frac{\gamma|\cos\theta|}{R\rho h d_H}} \quad (3)$$

where the hydrodynamic diameter of the microchannel, d_H, is defined as $4A/C$. For the luminol solution at the PDMS surface, γ, θ, and ρ are constant, while R, d_H, and h are determined by the design of the platform. Various types of CD-type microfluidic platforms with one variable (e.g., R) and two constant parameters (e.g., d_H and h) were fabricated. In order to verify eq. 3, a red-colored rose bengal solution (50 μM) was placed in the reservoir of a CD-type microfluidic platform, and the rotation speed of the turntable was increased in increments of 10 rpm. The behavior of the solution in the reservoir was observed with a high-speed charge-coupled device (CCD) camera (VW-Z1, Keyence, Co., Japan). The critical rotation speed, when the solution in the reservoir flowed out into another reservoir at the edge of the platform, was measured and the measurement was repeated three times.

Estimation of the performance of chemiluminescent signals on CD-type microfluidic platform

In order to evaluate the performance of the CD-type microfluidic platform for chemiluminescence detection under the rotation conditions, a 5-μL aliquot of an HRP solution at different concentrations (2, 5, 10, and 20 ppb) was placed in the reservoir of chemiluminescence sensing part at the edge of the platform. A 33-μL aliquot of a luminol solution was placed in the reservoir, which is located close to the center of the platform. The rotation speed of the turntable was then increased linearly up to 720 rpm to the elapse of time and then held constant at 720 rpm for 1 h. The chemiluminescent light was emitted by the reaction of HRP with the luminol solution, when the luminol solution flowed out from the reservoir to the sensing part at a critical rotation speed. The chemiluminescent signal was detected by the photon counting unit under the condition of a gating time of 2 s.

Preparation of anti-APnEOs antibody-immobilized magnetic microbeads

An anti-APnEOs antibody was immobilized on magnetic microbeads coated with polylactic acid by using an amino-coupling method [23]. The scheme for immobilization of the anti-APnEOs antibody on magnetic microbeads is shown in Fig. 3. A 200-μL suspension of microbeads (10 mg mL^{-1}) was placed in a microtube and washed with an imidazole-HCl buffer (pH = 7.0) several times. After washing, the volume of bead suspension was adjusted to 600 μL by adding the imidazole-HCl buffer. A 200-μL aliquot of EDC (0.8 M) and NHS (0.2 M) solutions were added to the tube, respectively, and the resulting suspension was incubated at 37 °C for 10 min in a thermostatic water bath. The microbeads were washed with the same imidazole-HCl buffer several times, and finally the supernatant liquid was removed. A 400-μL aliquot of an anti-APnEOs antibody solution (1 ppm) was added to the tube. The resulted suspension was incubated at 25 °C for 24 h in order to immobilize the antibody on the microbeads. The microbeads were then washed with a tris-HCl buffer (pH = 8.4) several times to block

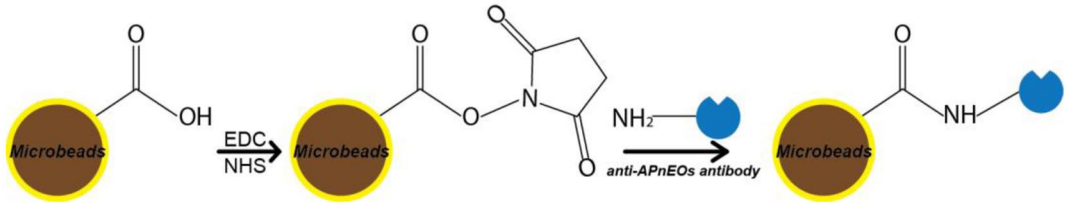

Fig. 3 Scheme of the immobilization of an anti-APnEOs antibody on magnetic microbeads coated with polylactic acid.

the unreacted esters on the microbeads. Finally, the volume of the suspension was adjusted to 1000 μL with the same tris-HCl buffer and the preparation was then stored in a refrigerator at about 2 °C. In order to examine the effect of the concentration of the anti-APnEOs antibody in the incubation solution on the amount of the antibody immobilized on the beads, anti-APnEOs antibody solutions at different concentrations (100–500 ppb) were also used for immobilization.

Estimation of amounts of anti-APnEOs antibody immobilized on magnetic microbeads

The anti-APnEOs antibody-immobilized magnetic microbeads prepared previously were allowed to react with an excess of the HRP-labeled APnEOs in order to estimate the amount of anti-APnEOs antibody immobilized on the magnetic microbeads. A 1000-μL aliquot of a 1 ppm HRP-labeled APnEOs solution was added to the microtube, which contained 0.4 mg of the anti-APnEOs antibody-immobilized magnetic microbeads. The resulting suspension was incubated at 25 °C for 30 min, and then washed with a phosphate-citric acid buffer (pH = 5.2) several times to remove traces of physically adsorbed HRP-labeled APnEOs on the surface of the microbeads and the microtube walls. The final volume of the suspension was adjusted to 50 μL with the same buffer solution. A 2 mg mL^{-1} *o*-phenylendiamine (OPD) solution (400 μL) and a 20 mM H_2O_2 solution (50 μL) were added to the microtube, and the resulted suspension was incubated at 25 °C for 30 min for color development. During this process, the OPD was oxidized to the product, 2,3-diaminophenylenazine (DAP), by reaction with H_2O_2 in the presence of HRP. After the incubation, 450 μL of the supernatant solution from the suspension was placed in another tube, and 450 μL of a H_2SO_4 solution (1.5 M) was added in order to terminate the color development reaction. The absorbance of the resulting solution was measured at a wavelength of 490 nm. The calibration curve of HRP-labeled APnEOs was obtained by measuring the absorbance of DAP resulting from the incubation between HRP-labeled APnEOs and the same composition of OPD and H_2O_2, as described above.

Chemiluminescence immunoassay for determination of APnEOs using CD-type microfluidic platform

A series of sample solutions were prepared by mixing an HRP-labeled APnEOs solution at a constant concentration (1000 ppb) and with different concentrations of an APnEOs solution (0, 2, 20, 100, 200, 1000, and 2000 ppb) at the same volume in a microtube. A 200-μL suspension containing 0.4 mg of the anti-APnEOs antibody-immobilized magnetic microbeads was added to the microtube containing a sample solution, and the resulted solution was then incubated at 25 °C for 30 min. The scheme for the present immunoassay is shown in Fig. 4. After incubation, the resulted magnetic microbeads were washed several times with a tris-HCl buffer (pH = 8.4) containing 0.1 % Tween 20, in order to remove traces of physically adsorbed HRP-labeled APnEOs on the surface of the microbeads. The magnetic microbeads were then placed in the sensing part on the CD-type microfluidic platform and trapped by the permanent magnet, which was fixed in the substrate platform at the same position. A 38-μL aliquot of a luminol solution containing H_2O_2 was placed in the reservoir, which was located close to the center of the platform. The CD-type platform was placed on the turntable, and the speed of rotation was gradually increased up to 720 rpm at a ramp of 10 rpm/s, and was then maintained constant at 720 rpm for 1 h. During the rotation, the chemiluminescent light emitted at the sensing part, where the magnetic microbeads were trapped, was detected by the photon counting unit under the condition of a gate time of 2 s.

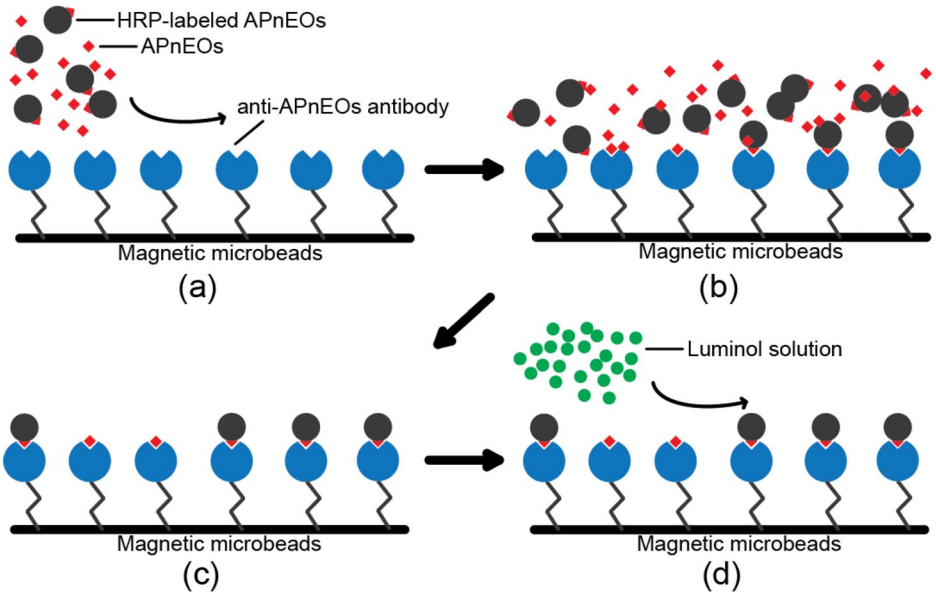

Fig. 4 Scheme of the protocol for immunoassay for the determination of APnEOs. (a) An anti-APnEOs antibody-immobilized magnetic microbeads was incubated with a sample solution containing APnEOs at different concentrations and HRP-labeled APnEOs at a constant concentration. (b) A competitive immunoreaction took place at the surface of the microbeads. (c) The microbeads were washed with a tris-HCl buffer (pH = 8.4) containing 0.1 % Tween 20 to remove the excess APnEOs and HRP-labeled APnEOs. (d) A luminol solution in the reservoir was sent to the sensing part where the microbeads were located by the centrifugal force resulting from the rotation of the CD-type platform by using a turntable, and the chemiluminescent emission was detected by a photon counting unit. Procedures (a) to (c) were performed in a microtube, and procedure (d) was performed on the CD-type microfluidic platform.

RESULTS AND DISCUSSION

Performance of CD-type microfluidic platform

Real-time videos of the rose bengal solutions in the reservoir were obtained with a high-speed CCD camera, and images of the solutions in the reservoir at a certain rotation speed were cut from the videos and are shown in Fig. 5. As the speed of rotation was increased, the solutions were forced to move to the bottom side of the reservoir by centrifugal force, and just before the solution in the reservoir flowed out from the outlet of the reservoir, the surface of the solution became flat and perpendicular to the outlet. Finally, at the critical rotation speed, the solution in the reservoir flowed out. As would be expected from eq. 1, the solution that was located at a longer distance from the center of the platform was subjected to a stronger centrifugal force, and the solution moved to the bottom side of the reservoir at a lower rotation speed. For example, a solution in reservoir No. 1 at a distance of 50 mm was moved to the bottom side of the reservoir at 967 rpm, while a solution in No. 5 at a distance of 25 mm moved to the bottom side at a much higher rotation speed of 1360 rpm. For solutions in each reservoir, when the speed of rotation increased to a certain value (critical rotation speed), the solution flowed out from the reservoir to another reservoir at the edge of the platform. For example, the critical rotation speeds for reservoirs Nos. 5 and 1 were 1405 rpm and 1013 rpm, respectively. The relationship between the critical rotation speed and the distance between the reservoir outlet and the center of the platform is shown in Fig. 6a. The solid line in Fig. 6a is the regression curve calculated from the experimental data by the Origin software program (Light Stone Co.). The observed critical rotation speeds are inversely proportional to the square root of the distance R, which agrees well with eq. 3. Other types of platforms with

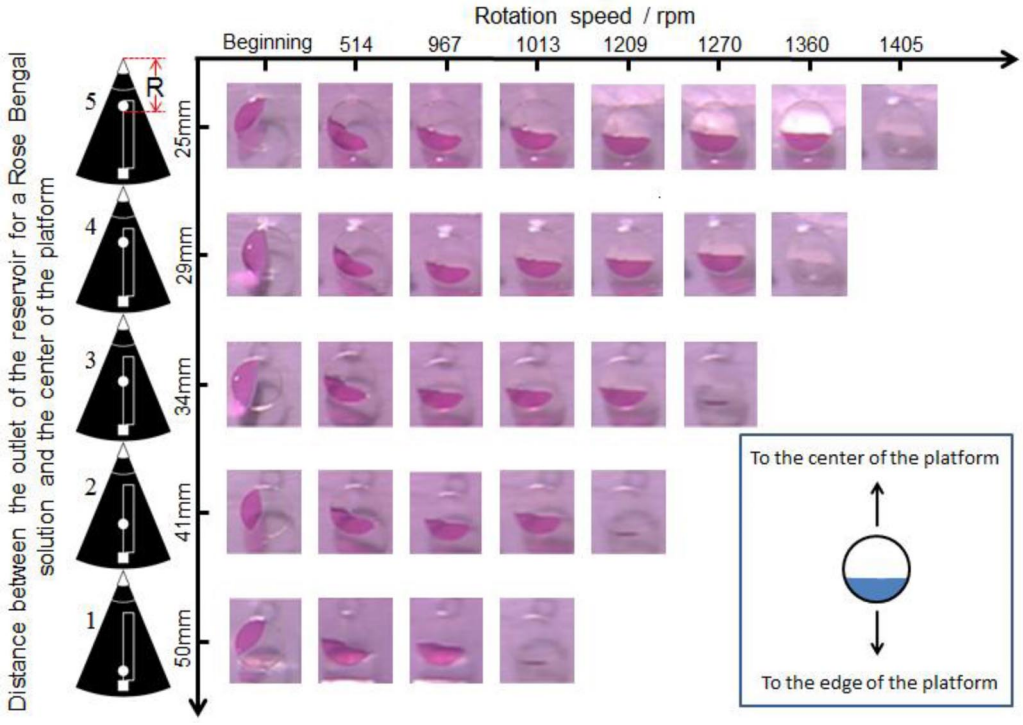

Fig. 5 Pictures of rose bengal solutions in the reservoirs at different rotation speeds. The pictures are cut from the real-time video taken with a high-speed CCD camera with 250 frame/s at a shutter speed of 10^{-4} s with the rotation speed increasing in increments of 10 rpm. The distances between the center of the platform and the outlets of the reservoirs from No. 1 to No. 5 were 50, 41, 34, 29, and 25 mm, respectively, and the reservoirs were 5 mm in diameter and 2 mm in depth. The width and depth of the microchannel were 500 and 40 μm, respectively. A 15-μL aliquot of the rose bengal solution was placed in the reservoir to give a solution height, h, of 2 mm. All of the sample solutions were placed at the left-side wall of the reservoir at the beginning and the platform was rotated in an anti-clockwise direction.

different channel sizes, d_H, or different solution heights, h, were also fabricated, and the critical rotation speed was measured in the same manner as above in order to verify eq. 3. The results are shown in Figs. 6b,c. The power indexes of the proportionality between the critical rotation speed and the channel size and the solution height are –0.50 and –0.45, respectively, as simulated by the experimental data. These two values are also in good agreement with values predicted from eq. 3. These results indicate that the fabricated CD-type microfluidic platform could be used to achieve a pump-free sequential flow at the selected rotation speed by adjusting the above parameters.

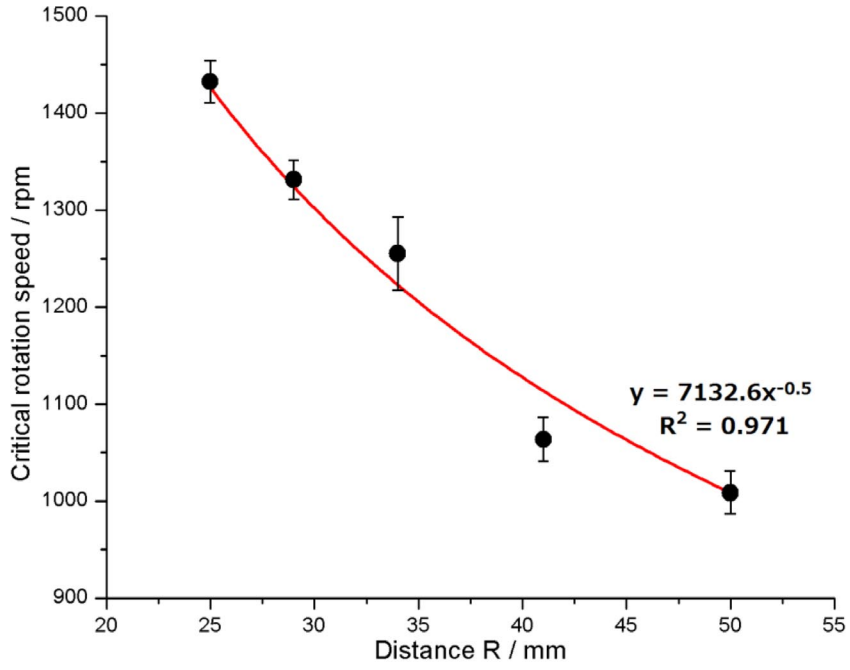

Fig. 6a Relationship between the critical rotation speed and the distance between the outlet of the reservoir and the center of the platform. *Solid lines denote the best fit for the curves with experimental data calculated using the Origin software program.

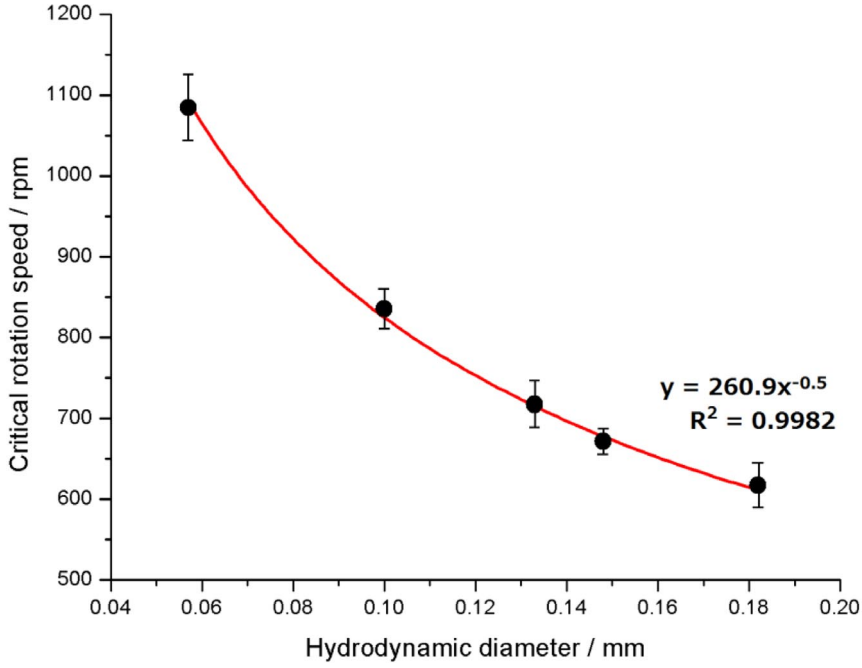

Fig. 6b Relationship between the critical rotation speed and the hydrodynamic diameter of the microchannel. The hydrodynamic diameter is defined as $4A/C$.

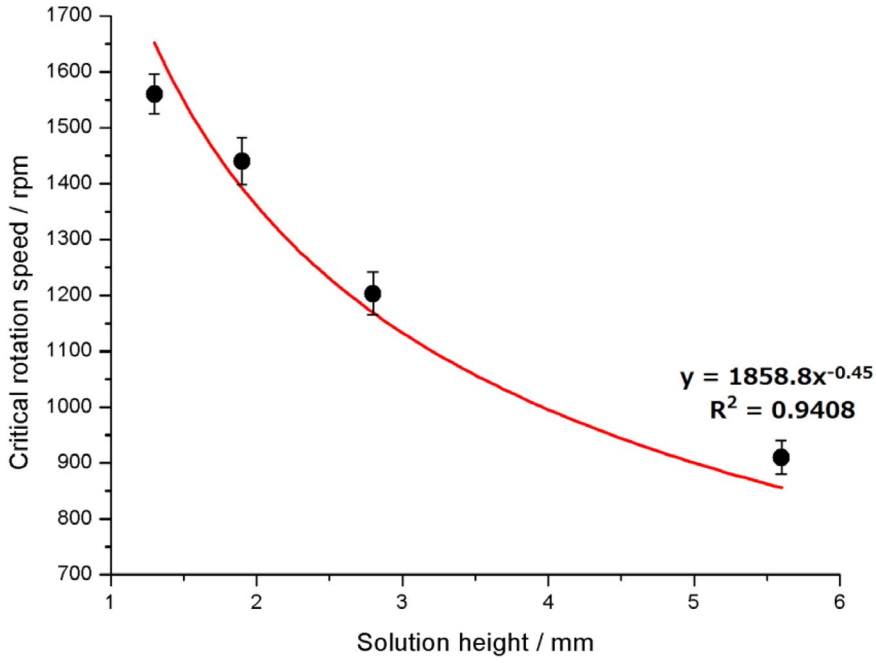

Fig. 6c Relationship between the critical rotation speed and the solution height in the reservoir.

Detection of chemiluminescent light by photon counting unit during the rotation of the CD-type microfluidic platform

In order to evaluate the performance of the system for detecting chemiluminescent light on the CD-type microfluidic platform, chemiluminescent light generated by the reaction of HRP with a luminol solution was detected using the photon counting unit during the rotation of the platform, using the set-up shown in Fig. 1. Figure 7a shows the change in the chemiluminescent intensity obtained at different ramps of rotation speed against time. The intensity of the chemiluminescence in the period from 0 to 60 s was determined to be about 50 photons per 2 s for a ramp of 10 rpm/s, which is the background level. This indicates that, during this period, the centrifugal force increased linearly with time, but was still lower than the surface tension, and the luminol solution therefore remained in the reservoir. At 60 s, when the rotation speed exceeded 600 rpm, the intensity of the chemiluminescent signals began to gradually increase, indicating that the luminol solution flowed into the sensing part, thus permitting the initiation of the chemiluminescence reaction. As estimated from Fig. 7a, as obtained in other experiments with different ramps, the critical speed of rotation, where the luminol solution in the reservoir flows out, is about 600 rpm.

Figure 7b shows the time course for the chemiluminescent signals when the platform was rotated up to 720 rpm with a ramp of 10 rpm/s. The chemiluminescent intensity began to increase steeply at about 60 s, and the maximum value was reached at about 400 s and then gradually decreased. The chemiluminescent intensity at the peak maximum obtained in these experiments with an average of 1370 photons/2 s were found to be fairly reproducible within 150 photons/2 s. Figure 7c shows the calibration curve obtained by plotting the peak value of chemiluminescent intensity against the concentration of the HRP solution located at the sensing part of the platform. The chemiluminescent signal is proportional to the concentration of the HRP solution in the range of 2–20 ppb, with a good correlation coefficient and reproducibility. This result indicates that the system used to detect the chemiluminescent signals from the rotating CD-type microfluidic platform performs sufficiently well that it can be used in a chemiluminescence immunoassay with good sensitivity and reproducibility.

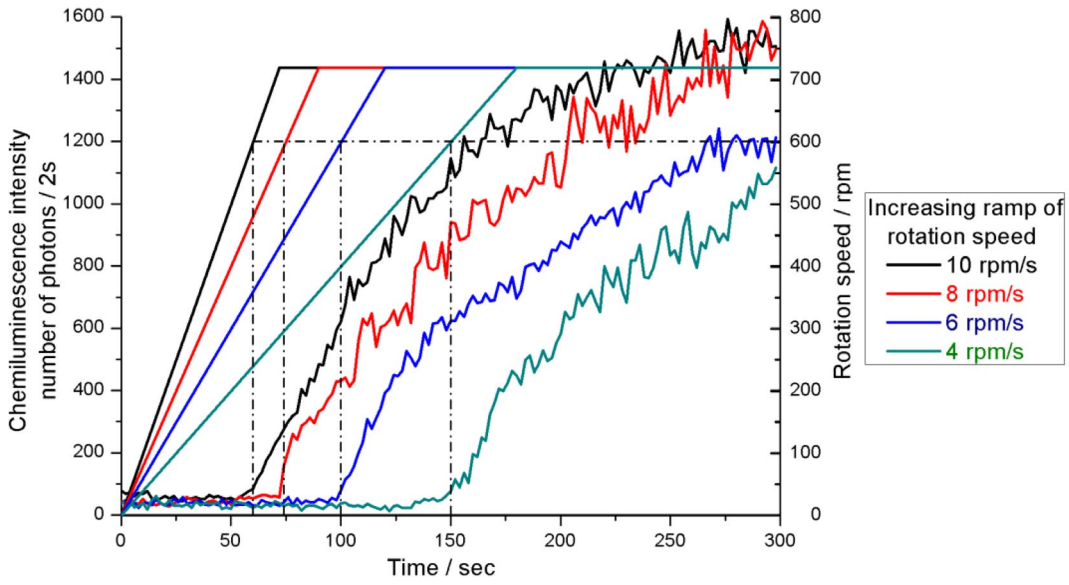

Fig. 7a Change in chemiluminescent signals under different ramps of rotation speed for a reaction of an HRP solution with a luminol solution at a sensing part on a platform. 5 μL of a 2 ppb HRP solution was placed in the sensing part, and a 33-μL aliquot of a luminol solution was placed in the reservoir located at 20 mm from the center. The microfluidic platform was rotated up to 720 rpm at different ramps of rotation speed, i.e., 4, 6, 8, and 10 rpm/s. After the rotation speed reached 720 rpm, the rotation speed was maintained constant at 720 rpm for a period of 300 s.

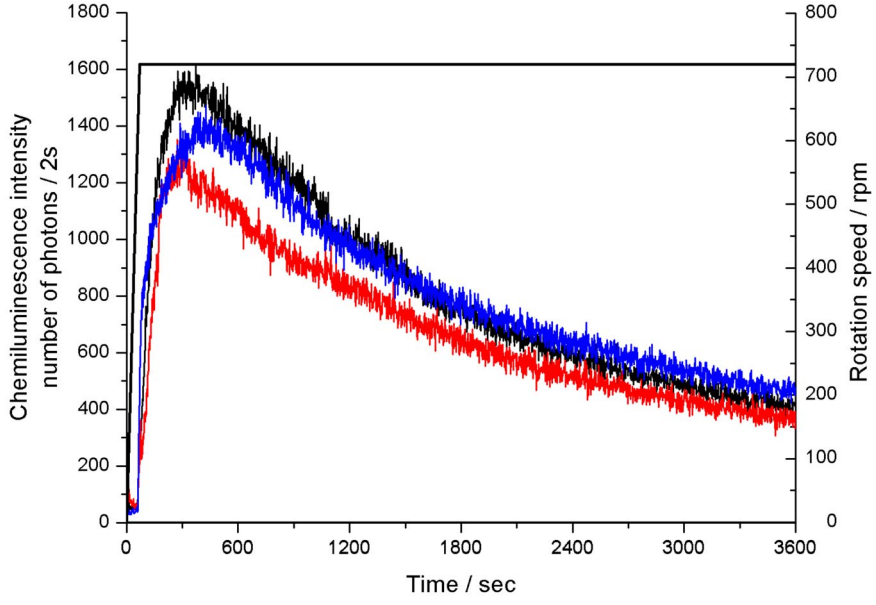

Fig. 7b The chemiluminescent signals produced when the luminol solution flowed into the sensing part where a 2 ppb HRP solution was located. The rotation speed was increased up to 720 rpm with a ramp of 10 rpm/s, and was then maintained constant at 720 rpm for 1 h.

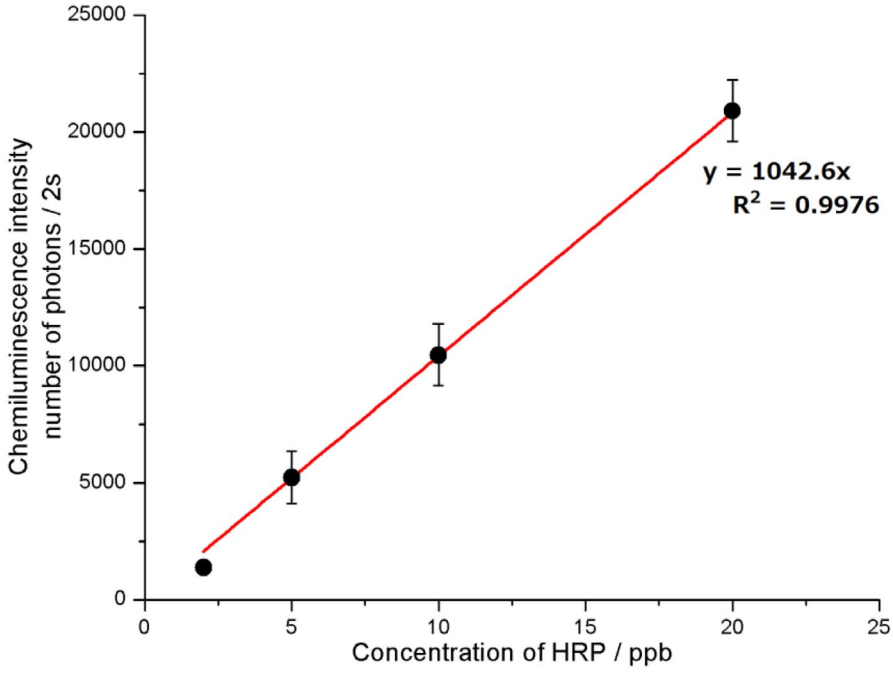

Fig. 7c Calibration curve of the HRP concentration in sample solutions plotted against the intensity of the chemiluminescent signals.

Estimation of amount of anti-APnEOs antibody immobilized on magnetic microbeads

Polylactic acid-coated magnetic microbeads were used as a solid support for immobilizing the anti-APnEOs antibody via an amino-coupling method. In order to estimate the amount of the antibody immobilized on the surface of the magnetic microbeads, the anti-APnEOs antibody-immobilized magnetic microbeads were reacted with an excess amount of a highly concentrated HRP-labeled APnEOs solution. It was assumed that the anti-APnEOs antibody immobilized on the surface of microbeads was completely bound to the HRP-labeled APnEOs, judging from the binding constant of the antibody with the HRP-labeled APnEOs, as described in the next section. After color development with OPD and H_2O_2, the amount of immobilized anti-APnEOs antibody was calculated from the absorbance of the resulting DAP solution, based on the calibration curve obtained from the color development reaction between the standard solutions of the HRP-labeled APnEOs and the same composition of OPD and H_2O_2 as we used in preliminary experiments.

Figure 8 shows the relationship between the amount of anti-APnEOs antibody immobilized on the magnetic microbeads and the concentration of anti-APnEOs antibody. As can be seen from Fig. 8, the amount of immobilized anti-APnEOs antibody increased monotonically with increasing concentration of anti-APnEOs antibody in the incubation solution in the concentration range from 100 to 500 ppb. The amount of anti-APnEOs antibody on the microbeads tends to become saturated in a concentration range higher than 500 ppb. When the concentration of the antibody was 1000 ppb, the amount of immobilized anti-APnEOs antibody was 0.75 μg/g-beads, which is comparable to the amount of anti-APnEOs antibody immobilized on the same type of magnetic microbeads used in our previous study (1.3 μg/g-beads) [23].

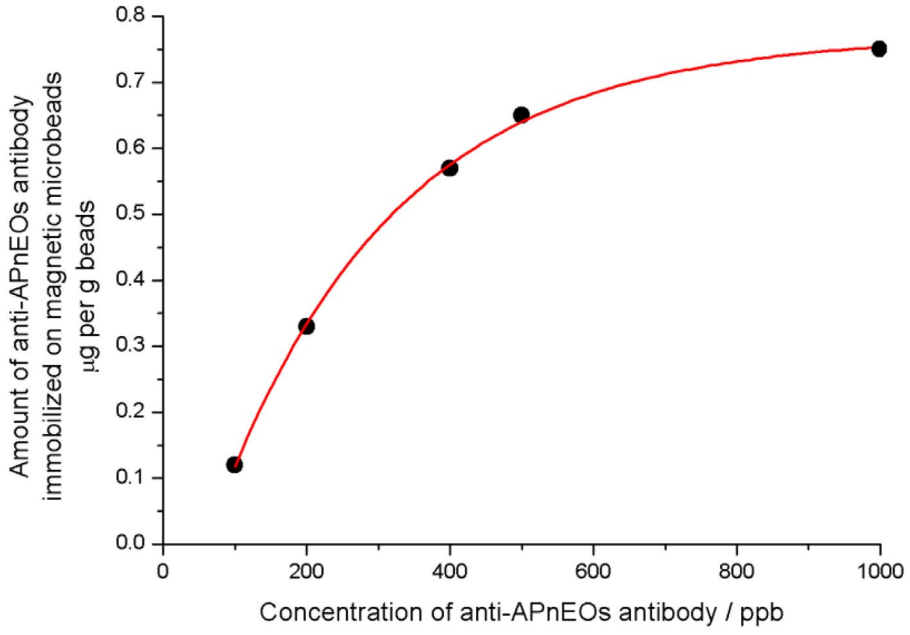

Fig. 8 Relationship between the amount of anti-APnEOs antibody immobilized on microbeads and the concentration of anti-APnEOs antibody used in the incubation solution.

Calibration curve of APnEOs

In our previous paper, a theoretical equation of the calibration curve of APnEOs for the same competitive immunoassay as the present work was derived and is expressed by eq. 4 [23].

$$\frac{[\underline{\text{Ab-HRP}\cdot\text{APnEOs}}]}{[\underline{\text{Ab}}]^{\text{T}}} = \frac{K_2 C_{\text{HRP}\cdot\text{APnEOs}}}{1 + K_1 C_{\text{APnEOs}} + K_2 C_{\text{HRP}\cdot\text{APnEOs}}} \tag{4}$$

where $[\underline{\text{Ab}}]^{\text{T}}$ and $[\underline{\text{Ab-HRP}\cdot\text{APnEOs}}]$ denote the total surface concentration of the anti-APnEOs antibody immobilized on the microbeads, and the surface concentration of the antibody-HRP-labeled-APnEOs conjugate, respectively. K_1 and K_2 are the binding constants of the anti-APnEOs antibody on the beads with APnEOs and the HRP-labeled APnEOs in the solution. C_{APnEOs} and $C_{\text{HRP}\cdot\text{APnEOs}}$ can be assumed to be the initial concentrations of APnEOs and the HRP-labeled APnEOs in the sample solutions, because these concentrations remain nearly unchanged after binding to the anti-APnEOs antibody on the beads, when the huge difference between the amount of anti-APnEOs antibody immobilized on the microbeads and the amount of the APnEOs and the HRP-labeled APnEOs in the sample solution are taken into consideration.

Figure 9a shows the time courses for the chemiluminescent signals produced as the result of the reaction of the luminol solution and HRP on the magnetic microbeads, which were incubated with sample solutions containing HRP-labeled APnEOs and APnEOs. As can be seen from Fig. 9a, the signals increased steeply after 60 s, when the luminol solution flowed out to the sensing part, and the intensities reach a maximum at about 1800 s, which was much slower than the change in the chemiluminescent signals shown in Fig. 7b. Also, as can be seen in Fig. 9a, the chemiluminescent signals decreased much more slowly than the change in the chemiluminescence shown in Fig. 7b. This is because in the experiment where the luminol solution flowed into the sensing part when the rotation speed exceeded 600 rpm and mixed efficiently with the HRP solution in the sensing part, the rate of the reaction was much higher compared with that in the experiment, in which the luminol solution reacted with HRP that

was conjugated on the surface of the microbeads that were trapped on the bottom wall of the sensing part.

Figure 9b shows calibration data for the APnEOs, in which the chemiluminescent intensities at the highest during 1 h are plotted against the concentration of APnEOs in the incubation solution with magnetic microbeads. In the present competitive immunoassay, the ratio of $[\underline{\text{Ab-HRP·APnEOs}}]/[\underline{\text{Ab}}]^{\text{T}}$ is proportional to the chemiluminescent signal, because the concentration of HRP on the microbeads is proportional to the chemiluminescent intensity, as shown in Fig. 7c. Therefore, the calibration data can be simulated using eq. 4 by selecting the binding constants K_1 and K_2 and using the concentration of the HRP-labeled APnEOs in the sample solution (500 ppb = 1.2×10^{-8} M), as a function of the concentration of APnEOs in the sample solution. The best fit for the theoretical calibration curve to the experimental data was obtained when K_1 and K_2 are 1.4×10^9 M^{-1} and 3.2×10^9 M^{-1}, respectively, as shown in Fig. 9b with a correlation coefficient of 0.987. According to the procedure for the immunoassay as the concentration of APnEOs reaches 80 % of the chemiluminescence signal, the detection limit of present method is ca. 10 ppb.

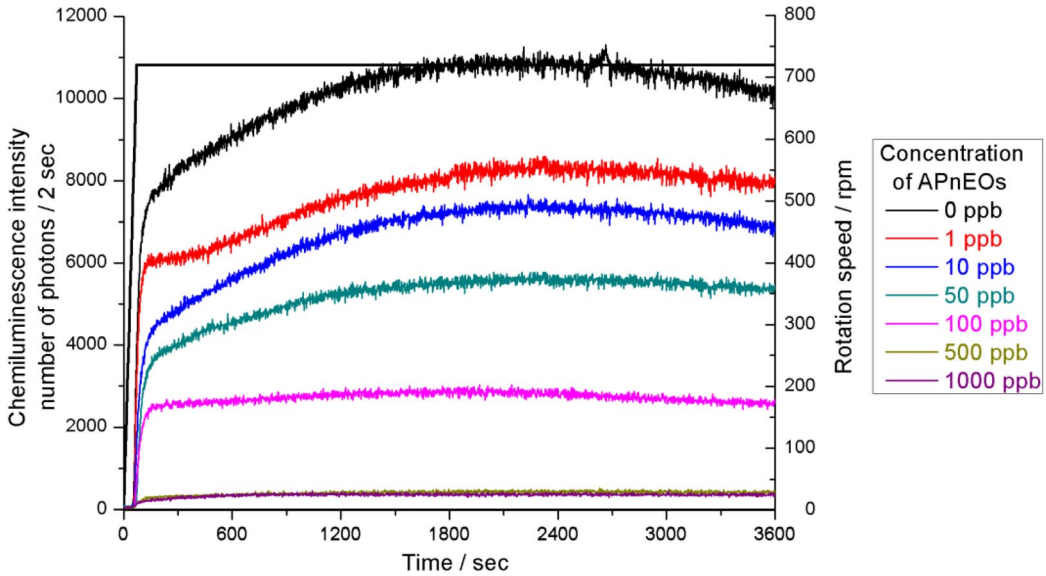

Fig. 9a The time course for the chemiluminescent signals produced from the reaction of luminol with HRP on magnetic microbeads incubated with the sample solutions containing HRP-labeled APnEOs (500 ppb) and APnEOs at different concentrations (0–1000 ppb). The rotation speed of the CD-type microfluidic platform was increased up to 720 rpm with a ramp of 10 rpm/s, and was then maintained constant at 720 rpm for 1 h.

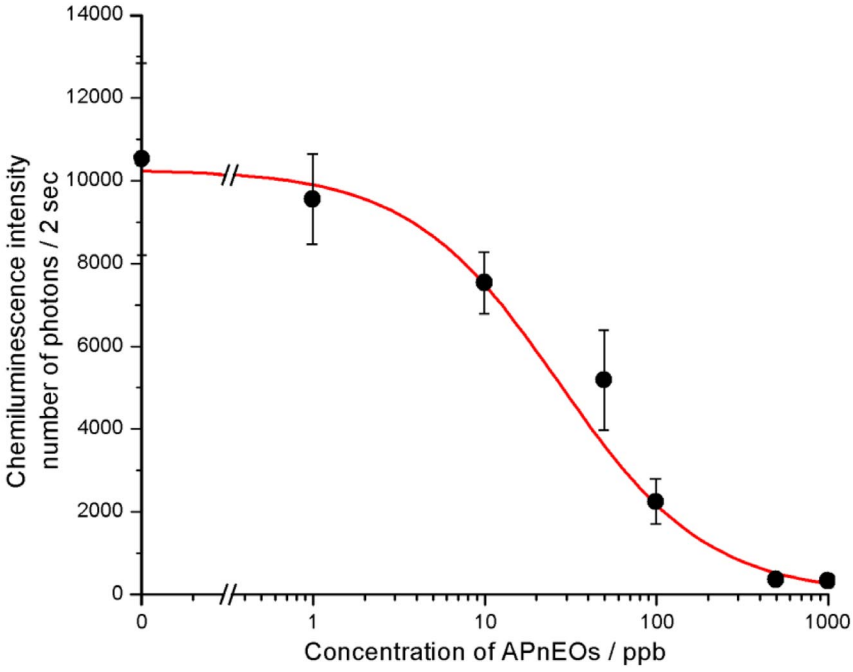

Fig. 9b Calibration curve based on chemiluminescent signals. Error bars are results from three repeated experiments. The solid line is the simulated calibration curve calculated from eq. 4, assuming $K_1 = 1.4 \times 10^9$ M^{-1}, and $K_2 = 3.2 \times 10^9$ M^{-1}.

CONCLUSION

We describe herein the development of a simple and pump-free chemiluminescence immunoassay for APnEOs that uses a CD-type microfluidic platform. The solutions in the reservoirs at different positions on the platform were delivered sequentially into the sensing part through a microchannel connected to each reservoir by appropriate adjustment of the speed of rotation of the platform. This is because the pumping function of the platform is based on developing a balance between centrifugal force and surface tension. Therefore, the sequential injection immunoassay for APnEOs reported previously [23] can be replaced by the CD-type microfluidic platform. However, at the present stage, the immunoreaction of the anti-APnEOs antibody immobilized on magnetic microbeads with APnEOs and HRP-labeled APnEOs was carried out in a test tube. This is due to an unsolved problem associated with the observance of a high background chemiluminescent signal when a sample solution and a washing solution located in appropriate reservoirs for sequential delivery. This may be due to the nonspecific adsorption of the HRP-labeled APnEOs on the sensing part, even if the sensing part is washed with the washing solution from a reservoir.

A semi-batch immunoassay can be achieved, simply by detecting the chemiluminescence on the microfluidic platform. The detection limit of the present method is almost the same order as that reported previously [23]. If the surface of the sensing part made from PDMS is modified with a hydrophilic coating, a completely pump-free sequential injection immunoassay can be achieved. The proposed system has the potential for use in monitoring environmental and sewage treatment water.

ACKNOWLEDGMENTS

The authors wish to acknowledge financial support from the Global COE Program "Science for Future Molecular Systems" from the Ministry of Education, Culture, Sports, Science and Technology (MEXT) of Japan.

REFERENCES

1. A. V. Barse, T. Chakrabarti, T. K. Ghosh, A. K. Pal, S. B. Jadhao. *Pestic. Biochem. Physiol.* **86**, 172 (2006).
2. T. Vega Morales, M. E. Torres Padrón, Z. Sosa Ferrera, J. J. Santana Rodríguez. *Trends Anal. Chem*. **28**, 1186 (2009).
3. M. Jontofsohn, M. Stoffels, A. Hartmann, G. Pfister, I. Juttner, G. Severin-Edmair, K.-W. Schramm, M. Schloter. *Sci. Total Environ*. **285**, 3 (2002).
4. J. Montgomery-Brown, J. E. Drewes, P. Fox, M. Reinhard. *Water Res.* **37**, 3672 (2003).
5. B. Gross, J. Montgomery-Brown, A. Naumann, M. Reinhard. *Environ. Toxicol. Chem.* **23**, 2074 (2004).
6. M.-L. Janex-Habibi, A. Huyard, M. Esperanza, A. Bruchet. *Water Res.* **43**, 1565 (2009).
7. I. Tubau, E. Vazquez-Sune, J. Carrera, S. Gonzalez, M. Petrovic, M. J. L. Alda, D. Barcelo. *J. Hydrol.* **383**, 102 (2010).
8. R. Espejo, K. Valter, M. Simona, Y. Janin, P. Arrizabalaga. *J. Chromatogr., A* **976**, 335 (2002).
9. C. Y. Cheng, W. R. Li, J. W. Chang, H. C. Wu, W. H. Ding. *J. Chromatogr., A* **1127**, 246 (2006).
10. V. Andreu, E. Ferrer, J. L. Rubio, G. Font, Y. Pico. *Sci. Total Environ.* **378**, 124 (2007).
11. P. A. Lara-Martin, A. Gomez-Parra, E. Gonzalez-Mazo. *J. Chromatogr., A* **1137**, 188 (2006).
12. M. Cantero, S. Rubio, D. Perez-Bendito. *J. Chromatogr., A* **1046**, 147 (2004).
13. Y. K. K. Koh, T. Y. Chiu, A. R. Boobis, E. Cartmell, S. J. T. Pollard, M. D. Scrimshaw, J. N. Lester. *Chemosphere* **73**, 551 (2008).
14. S. Banerjee. *Anal. Chem.* **57**, 2590 (1985).
15. A. Marcomini, S. Capri, W. Giger. *J. Chromatogr.* **403**, 243 (1987).
16. A. Marcomini, W. Giger. *Anal. Chem.* **59**, 1709 (1987).
17. J. F. Liu, X. Liang, G. B. Jiang, Y. Q. Cai, Q. X. Zhou, G. G. Liu. *J. Sep. Sci.* **26**, 823 (2003).
18. T. Takasu, A. Iles, K. Hasebe. *Anal. Bioanal. Chem.* **372**, 554 (2002).
19. H. Sato, A. Shibata, Y. Wang, H. Yoshikawa, H. Tamura. *Biomacromolecules* **4**, 46 (2003).
20. D. Norton, S. A. Shamsi. *Anal. Chem.* **79**, 9459 (2007).
21. Y. Goda, A. Kobayashi, S. Fujimoto, Y. Toyoda, K.-I. Miyagawa, M. Ike, M. Fujita. *Water Res.* **38**, 4323 (2004).
22. K. Nishi, Y. Goda, S. Fujimoto, H. Inui, H. Ohkawa. *Mol. Immunol.* **46**, 3125 (2009).
23. R. Zhang, H. Nakajima, N. Soh, K. Nakano, T. Masadome, K. Nagata, K. Sakamoto, T. Imato. *Anal. Chim. Acta* **600**, 105 (2007).
24. J. Steigert, T. Brenner, M. Grumann, L. Riegger, S. Lutz, R. Zengerle, J. Ducree. *Biomed. Microdevices* **9**, 675 (2007).
25. M. Yamada, K. Kano, Y. Tsuda, J. Kobayashi, M. Yamato, M. Seki, T. Okano. *Biomed. Microdevices* **9**, 637 (2007).
26. M. Grumann, J. Steigert, L. Riegger, I. Moser, B. Enderle, K. Riebeseel, G. Urban, R. Zengerle, J. Ducree. *Biomed. Microdevices* **8**, 209 (2006).
27. H. Kido, M. Micic, D. Smith, J. Zoval, J. Norton, M. Madou. *Colloids Surf., B* **58**, 44 (2007).
28. S. Furutani, H. Nagai, Y. Takamura, I. Kubo. *Anal. Bioanal. Chem.* **398**, 2997 (2010).
29. C. Li, X. Dong, J. Qin, B. Lin. *Anal. Chim. Acta* **640**, 93 (2009).
30. R. Peytavi, F. R. Raymond, D. Gagne, F. J. Picard, G. Jia, J. Zoval, M. Madou, K. Boissinot, M. Boissinot, L. Bissonnette, M. Ouellette, M. G. Bergeron. *Clin. Chem.* **51**, 1836 (2005).

31. G. Jia, K. Ma, J. Kim, J. V. Zoval, R. Peytavi, M. G. Bergeron, M. Madou. *Sens. Actuators, B* **114**, 173 (2006).
32. X. Y. Peng, P. C. H. Li, H.-Z. Yu, M. Parameswaran, W. L. Chou. *Sens. Actuators, B* **128**, 64 (2007).
33. N. Honda, U. Lindberg, P. Andersson, S. Hoffmann, H. Takei. *Clin. Chem.* **51**, 1955 (2005).
34. S. Lai, S. Wang, J. Luo, L. J. Lee, S. Yang, M. Madou. *Anal. Chem*. **76**, 1832 (2004).
35. L. Riegger, M. Grumann, T. Nann, J. Riegler, O. Ehlert, W. Bessler, K. Mittenbuehler, G. Urban, L. Pastewka, T. Brenner, R. Zengerle, J. Ducree. *Sens. Actuators, A* **126**, 455 (2006).
36. C. Li, H. Li, J. Qin, B. Lin. *Electrophoresis* **30**, 4270 (2009).
37. J. Steigert, M. Grumann, M. Dube, W. Streule, L. Riegger, T. Brenner, P. Koltay, K. Mittmann, R. Zengerle, J. Ducree. *Sens. Actuators, A* **130**, 228 (2006).

